Current Biology, Vol. 15, 1413–1419, August 9, 2005, ©2005 Elsevier Ltd All rights reserved. DOI 10.1016/j.cub.2005.06.058

The Homeobox Transcription Factor Even-skipped Regulates Netrin-Receptor Expression to Control Dorsal Motor-Axon Projections in *Drosophila*

Juan Pablo Labrador,[1] David O'Keefe,[2] Shingo Yoshikawa,[2] Randall D. McKinnon,[3] John B. Thomas,[2] and Greg J. Bashaw[1,*]
[1]Department of Neuroscience
University of Pennsylvania School of Medicine
421 Curie Boulevard
Philadelphia, Pennsylvania 19104
[2]Molecular Neurobiology Laboratory
Salk Institute for Biological Studies
P.O. Box 85800
San Diego, California 92186
[3]Departments of Surgery and
Molecular Genetics Microbiology
Robert Wood Johnson Medical School
675 Hoes Lane
Piscataway, New Jersey 08854

Summary

Homeobox transcription-factor codes control motor-neuron subtype identity and dorsal versus ventral axon guidance in both vertebrate and invertebrate nervous systems [1–4]; however, the specific axon guidance-receptors that are regulated by these transcription factors to control pathfinding are poorly defined. In *Drosophila*, the Even-skipped (Eve) transcription factor specifies dorsal motor-axon projection [5] through the regulation of unidentified guidance molecules. The Netrins and their attractive and repulsive receptors DCC and Unc-5, respectively, define important conserved cue and receptor families that control growth-cone guidance [6]. In *Drosophila*, the Netrins and *frazzled* (the fly homolog of DCC) contribute to motor-axon guidance [7–9]. Here, using genetics and single-cell mRNA-expression analysis, we show that expression and requirement of different Netrin receptor combinations correlate with distinct dorsal and ventral motor-axon projections in *Drosophila*. Misexpression of *eve* dorsalizes ventral axons in part through the upregulation of *Unc-5*, whereas loss of *eve* function in two dorsally projecting motor neurons results in aberrant axon projections and a failure to express *Unc-5*. Our results support a functional link between the expression of distinct Netrin receptor combinations and the transcriptional control of dorsal motor-axon guidance.

Results and Discussion

Unc-5 Mutants Display Multiple Defects in Motor-Axon Guidance

Genetic analysis indicates that the *Drosophila* Netrins (NetA and NetB) and the attractive Netrin receptor Fra guide subsets of embryonic motor axons [7–9]. Specifically, *NetAB* double mutants affect multiple motor projections, including the dorsally projecting intersegmental nerve (ISN), the laterally projecting segmental nerve (SN), and the ventrally projecting ISNb [7, 9], whereas *fra* mutants disrupt the dorsal ISN and the ventral ISNb [8]. In contrast to attraction mediated by DCC/Fra/Unc-40 receptors, Unc-5 receptors mediate repulsion [10–12]. Unc-5 can act either independently or together with DCC to mediate Netrin repulsion [13–15]. Previous studies of *Unc-5* in *Drosophila* have examined the effects of mis- and overexpression of *Unc-5* [10]. Analysis of endogenous *Unc-5* function has been limited to RNA interference (RNAi) approaches, where *Unc-5* function was reduced in embryos overexpressing *NetB*. In these experiments, *Unc-5* RNAi partially suppresses the gain-of-function *NetB* phenotype, suggesting that *Unc-5* functions as a repulsive Netrin receptor [10].

To further address the endogenous role of *Unc-5*, we have generated mutations in *Unc-5* and examined their effects on motor-axon guidance in *Drosophila* embryos (see Supplemental Experimental Procedures and Tables S1 and S2 in the Supplemental Data available with this article online). Before describing the defects in *Unc-5* mutants, it is useful to review the phenotypes observed in *NetAB* double mutants and *fra* mutants [7–9, 16]. *NetAB* and *fra* mutants both affect the trajectory of the ISN, which normally projects dorsally past the epidermal stripe of NetA expression to innervate dorsal muscles (Figure 1A). Specifically, the ISN is observed to inappropriately (1) stall, (2) branch excessively, (3) cross segment boundaries, and (4) project beyond the dorsal target muscles (Figures 1B and 1D). Both *NetAB* and *fra* mutants also frequently disrupt the normal ventral ISNb innervation of the NetB expressing muscles 6 and 7 (Figures 1B and 1D). In addition, lateral SNa axon projections are disrupted in *NetAB* double mutants. In wild-type, SNa projects to the lateral muscle field, where it bifurcates to innervate muscles 5 and 8 and transverse muscles 21, 22, 23, and 24 (Figure 1A). In *NetAB* double mutants, SNa sometimes stalls or is missing one of the two major branches (Figure 1B). We do not see these phenotypes in *fra* mutants (Figure 1D), suggesting that Netrin's influence on SNa guidance is *fra*-independent. This finding is consistent with previous observations that the *NetB* gain-of-function phenotype in SNa is *fra*-independent [16].

Loss of *Unc-5* function results in defects that overlap with the phenotypes observed in *fra* and *NetAB* mutants (Figure 1C). Specifically, in *Unc-5* mutants, like in *NetAB* and *fra* mutants, the dorsally projecting ISN inappropriately crosses the segment boundary (Figure 1C). The *Unc-5* ISN defects are observed at similar frequency to *NetAB* and at a higher frequency than *fra*, which consistently shows weaker ISN crossover phenotypes (Figure 1E). We interpret these phenotypes as a failure to be repelled by the epidermal stripe of NetA expression (Figure 1B). In contrast to *fra*, where the SNa is not affected, *Unc-5* mutants display SNa defects that are qualitatively similar to those observed in *NetAB*, including premature stalling and absence of one or both branches (Figure 1C). This suggests that Netrin influence on SNa guidance represents a repul-

*Correspondence: gbashaw@mail.med.upenn.edu

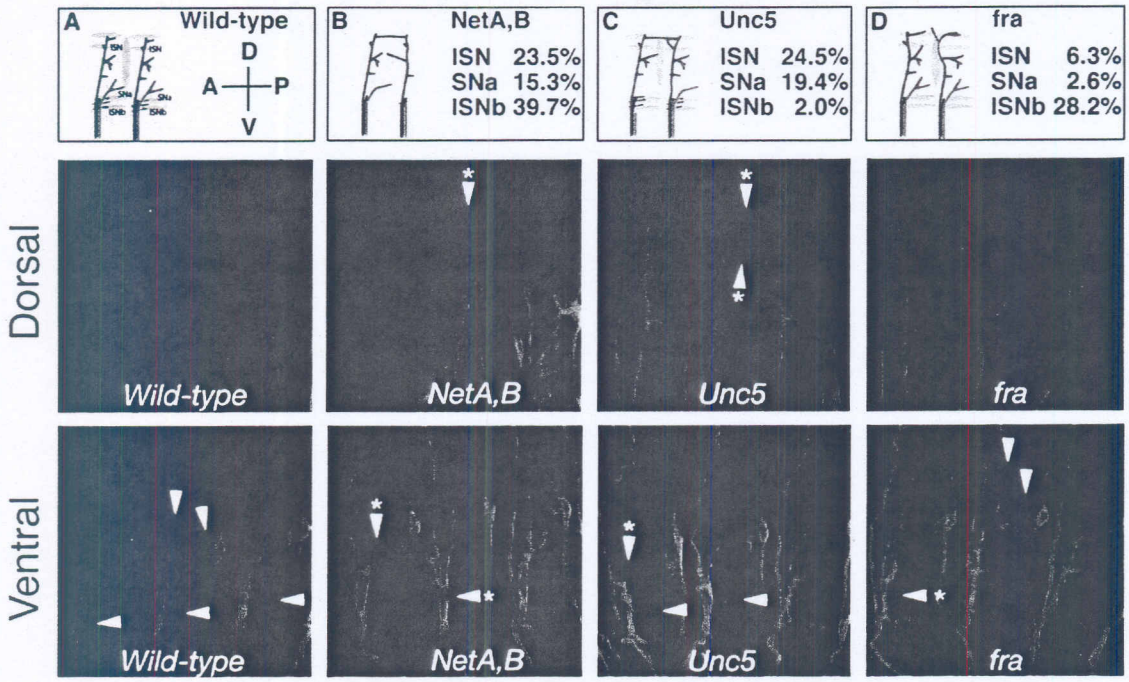

Figure 1. Motor-Axon-Guidance Defects in *NetAB, fra*, and *Unc-5* Mutants

Stage-17 embryos stained with anti-FasII Mab to reveal the motor projections. Images represent the maximum projection of confocal stacks to reveal all projections in a single focal plane. Anterior is left and dorsal is up in all panels. Three adjacent abdominal hemisegments are shown. Partial genotypes are indicated below each panel. Top panels are schematic representations of the wild-type and mutant-motor-axon projections. Middle panels show the more dorsal projections, and bottom panels show the more ventral projections.

(A) Wild-type. The top panel indicates the normal projections of the ISN, SNa, and ISNb as well as the domain of Netrin expression. For simplicity, NetA and NetB expression are combined and shown as shaded ovals. Netrin is expressed in a presumptive gradient from the CNS midline (not shown), in ventral muscles 6 and 7, in a more lateral epidermal stripe, and in dorsal muscles 1 and 2. Note the normal trajectory of the ISN as it projects dorsally and respects the segment boundary (middle panel).

(B–D, middle panels) The ISN can be seen inappropriately crossing the segment boundary and fasciculating with the ISN in neighboring segments (arrows with asterisks). *NetAB* double mutants exhibit defects in 23.5% ± 3.3% of all segments examined (B), and *Unc-5* mutants exhibit defects in 24.5% ± 3.5% of all segments examined (C). The ISN defects are observed less frequently in *fra* mutants, where defects were exhibited in 6.3% ± 1.8% of all segments examined (D).

(A, bottom panel) Wild-type. The SNa and ISNb nerve branches are indicated. Note the two branches of the SNa as they make appropriate contacts with their target muscles (arrowheads). The normal innervation of muscles 6 and 7 by the ISNb is also indicated (arrowheads).

(B–D, bottom panels) In *NetAB* double mutants (B), and *Unc-5* mutants (C), one or both of the SNa branches are sometimes missing (arrowheads with asterisks). *NetAB* double mutants and *Unc-5* mutants exhibit these SNa defects in 15.3% ± 4.3% and 19.4% to 28.2% ± 3.9% of all segments examined, respectively. In contrast, in *fra* mutants (D), SNa innervations are normal (arrowheads). In *NetAB* double mutants (B) and *fra* mutants (D), the ISNb innervation of muscles 6 and 7 is often absent (arrowheads with asterisks). *NetAB* double mutants and *fra* mutants exhibit this ISNb phenotype in 39.7% and 28.2% of all segments examined, respectively. In *Unc-5* mutants (C), ISNb innervations are normal (arrowheads).

sive function. Finally, in contrast to *NetAB* and *fra*, ISNb guidance is normal in *Unc-5* mutants (Figure 1C), suggesting an attractive role of *NetAB* and *fra* in regulating ISNb guidance. Importantly, the ISN and SNa guidance defects observed in *Unc-5* mutants can be rescued by expressing *Unc-5* in neurons, indicating that *Unc-5* functions cell autonomously in motor neurons during their guidance (Figure S1).

In summary, loss of *NetAB* function results in three categories of motor-axon phenotypes: (1) phenotypes that depend on both *Unc-5* and *fra* (dorsal ISN), (2) phenotypes dependent on *Unc-5* but not *fra* (lateral SNa), and (3) phenotypes dependent on *fra* but not *Unc-5* (ventral ISNb). These data suggest that different receptor combinations are required for the guidance of different subsets of axons. Moreover, there is a clear correlation between the relative dorsal/ventral projection pattern of motor neurons and the genetic requirement for different receptor combinations.

Differential Expression of *Unc-5* and *fra* in Subsets of Motor Neurons

We next investigated the possibility that neurons with differential genetic requirements for *Unc-5* and *fra* may show differential expression of the receptors. To examine expression patterns of *Unc-5* and *fra* in specific dorsal, lateral and ventral motor neurons, we labeled embryos with fluorescent-RNA in situ probes and simultaneously detected protein markers that define dorsally projecting ISN motor neurons (*RN2Gal4* driving *UASTauMycGFP* [*RN2TMG*]) [17], laterally projecting SN motor neurons (FasII) [18], and ventrally projecting

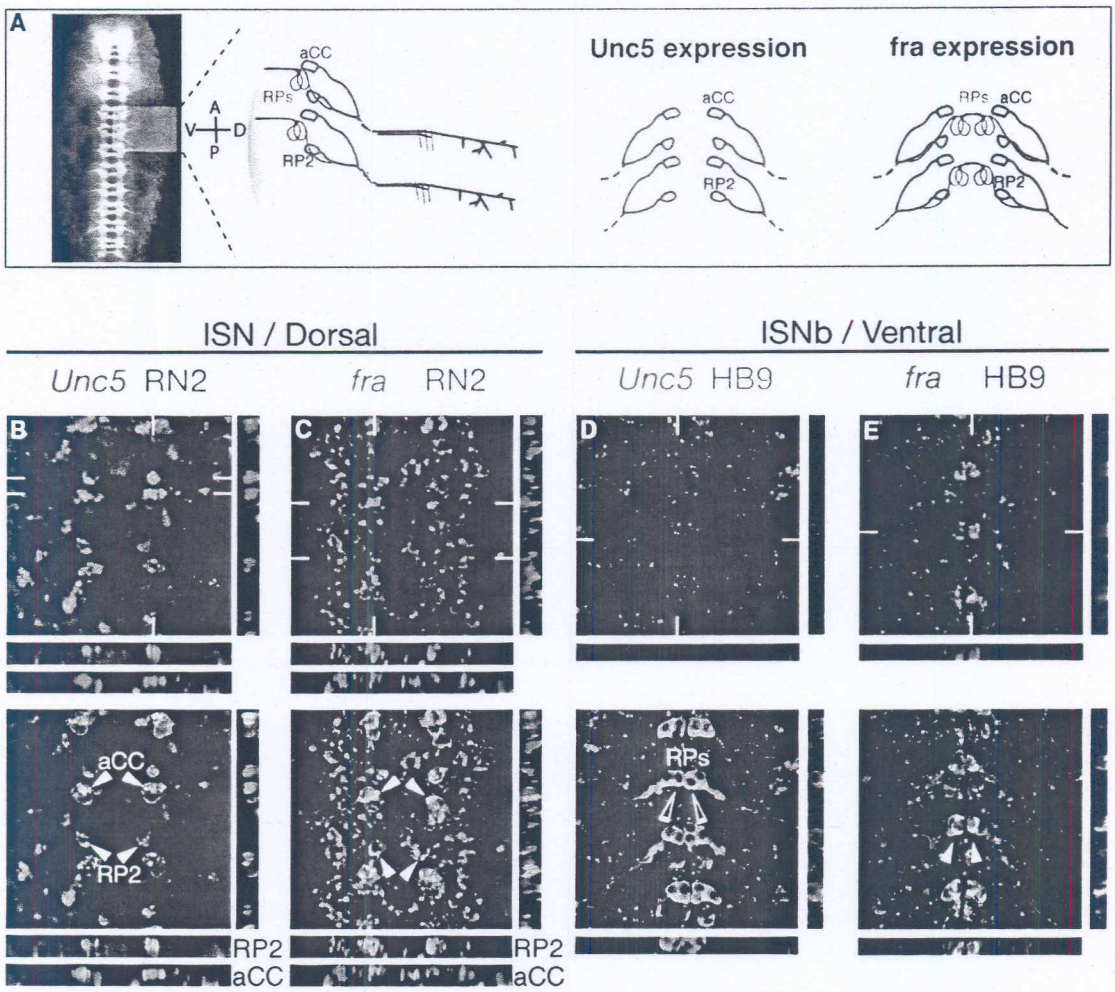

Figure 2. *Unc-5* and *fra* mRNA-Expression Patterns in Defined Motor Neurons

(A) A schematic diagram summarizing the positions of cells and the expression of *fra* and *Unc-5* for the dorsally projecting motor neurons labeled by RN2Gal4 (aCC and RP2 are colored blue) and some of the ventrally projecting neurons labeled by HB9Gal4 (RPs are colored red). (B–E) Stage-13 RN2Gal4::TauMycGFP embryos (B and C) or stage-17 dHb9Gal4::TauMycGFP embryos (D and E) were double labeled with RNA in situ probes for either *Unc-5* (B and D) or *fra* (C and E) and antibodies to GFP to examine defined motor neurons. The top panels show RNA signals in green, and the bottom panels show the overlay of the RNA (green) and protein signals (red). Anterior is up in all panels. White hash marks in the in situ panels indicate the positions of the XZ and YZ sections displayed below and to the right of the main XY panels, respectively. In (B and C), two separate XZ sections are shown, one for aCC and one for RP2. (B) *Unc-5* is expressed in both the aCC and RP2 motor neurons (arrowheads). (C) *fra* is also expressed in aCC and in RP2 (arrowheads). (D and E) A dorsal (internal) layer of stage-17 embryos stained with anti-GFP to reveal some of the midline RP neurons, and either *Unc-5* in situ probe (D) or *fra* in situ probe (E) shows that the midline RP neurons express *fra* (arrowheads in E) but not *Unc-5* (empty arrowheads in D). Note the clear localization of both *unc-5* and *fra* in aCC and RP2 in the XZ and YZ sections (B and C) and the localization of *fra* but not *Unc-5* in the midline RP neurons in the XZ and YZ sections (D and E).

ISNb motor neurons (*HB9Gal4* driving *UASTauMycGFP* [*Hb9TMG*]) [19]. In addition to labeling axons, these markers clearly label neuronal cell bodies, allowing us to determine whether the *fra* and *Unc-5* mRNAs are specifically expressed in these neurons (Figure 2). Here, it is critical to use fluorescence mRNA in situ, rather than antibody staining, to detect receptor expression because antibody staining does not allow us to resolve which individual neurons express the receptors.

Double labeling of stage-13 embryos with *RN2TMG* and *Unc-5* or *fra* mRNA probes shows that both receptors are expressed by the RP2 and aCC neurons, pioneers of the ISN (Figures 2A–2C). Both receptors are also clearly expressed in additional cells not labeled by our protein markers, with *fra* showing a considerably broader expression pattern than *Unc-5*. Expression of *fra* and *Unc-5* in the ISN is consistent with phenotypes of the *fra* and *Unc-5* mutants and suggests that the ISN-guidance defects may reflect a loss of Netrin repulsion rather than a loss of attraction, which had been previously inferred from the similarity of *fra* and *NetAB* mutants [8]. Interestingly, and consistent with the inability to detect Unc-5 protein on the ISN in late-stage embryos [10], *Unc-5* mRNA expression in aCC and RP2

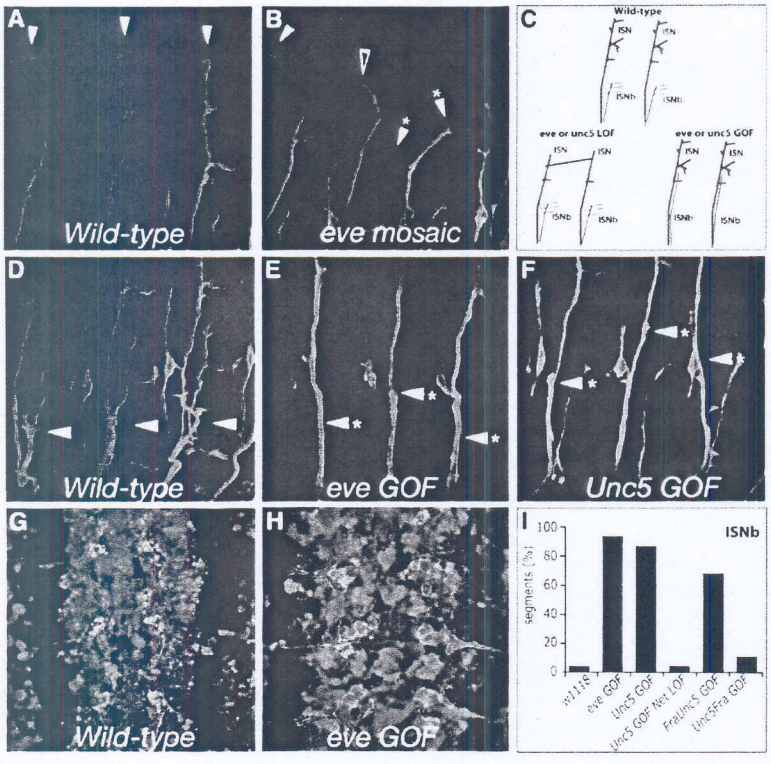

Figure 3. Comparison of *eve* and *Unc-5* Loss- and Gain-of-Function Phenotypes

Stage-17 embryos (dorsal is up and anterior is left) (A–F) and stage-13 embryos ventral views (G and H) stained with MAb Fas II to reveal motor projections (A–F) or double labeled with MAb FasII and *Unc-5* mRNA in situ probe to visualize motor projections and *Unc-5* mRNA (G and H). Partial genotypes are indicated below each panel. GOF denotes gain of function. LOF denotes loss of function.

(A) Wild-type dorsal motor-axon projections.

(B) In *eve* mosaic mutants, dorsal projections show multiple defects including abnormally short projections (31%) (empty arrowheads), bifurcations (20%), and inappropriate crossing of segment boundaries (20%) (arrowheads with asterisks).

(C) A schematic representation of the loss- and gain-of-function *eve* and *Unc-5* mutant phenotypes in the dorsal-ISN and ventral-ISNb motor branches. *eve* mosaic and *Unc-5* loss of function frequently result in inappropriate crossing of the segment boundary by the ISN. *eve* and *Unc-5* gain of function both result in abnormal dorsal projection of the ventral ISNb.

(D) Wild-type ventral motor-axon projections.

(E) Misexpressing *eve*, (*UASeve, ElavGal4*) results in aberrant dorsal projection of both ventral-ISNb and lateral-SNa branches, which can be seen fasciculating with the ISN in each of the three hemisegments pictured (arrowheads with asterisks).

(F–I) A *UASHA-Unc-5, ElavGal4* embryo is shown in (F). The ventral-ISNb branch has joined the dorsal ISN and projects dorsally (arrowheads with asterisks); note the increased thickness of the ISN relative to the wild-type embryo in (A) and (D). The SNa is not affected. In wild-type embryos, *Unc-5* mRNA is detected in a small number of cells including aCC (G), whereas in *UASeve, ElavGal4* embryos, many additional cells express *Unc-5* mRNA (H). The heterogeneity in the elevation of *Unc-5* mRNA levels suggests that *eve* alone is not completely sufficient to positively regulate *Unc-5*. (I) shows quantification of phenotypes. Genotypes are indicated on the x axis, percentages of segments showing defects in the normal ventral projection of the ISNb are indicated on the y axis (wild-type, 5.5% ± 0.5%, n = 36; *eve* misexpression, 96.7% ± 0.5%, n = 32; *Unc-5* misexpression, 90.3% ± 0.8%, n = 72; *Unc-5* misexpression in the *NetAB* mutant background, 5.9% ± 0.7%, n = 68*; *FraUnc-5* misexpression, 68.7% ± 1.6%, n = 48; and *Unc-5Fra*, 10% ± 1.1%, n = 80). Data shown are ± standard error of the mean (SEM).

*As expected, *NetAB* mutant embryos that misexpress *Unc-5* exhibit the characteristic failure of muscle-6 and -7 innervation normally seen in *NetAB* double mutants.

is significantly reduced in late-stage embryos when ISN should be forming synapses on dorsal muscles 1 and 2 (Figure S2). Whether or not the downregulation of *Unc-5* in older embryos is required for guidance or targeting to the dorsal muscles in wild-type animals is an open question; however, the observation that ISN guidance appears relatively normal in embryos that ectopically express *Unc-5* would suggest that the observed downregulation is not important for proper guidance.

FasII analysis of laterally projecting neurons in stage-13 animals shows that at least one of the SN neurons, identified by shape, position, and projection as it exits to the muscle field [20], expresses *Unc-5* but not *fra* (J.-P.L. and G.J.B., unpublished data). Consistent with this observation, previous studies have shown that Unc-5 protein is expressed in the SNa [10]. Finally, double labeling of stage-17 embryos with *HB9TMG* and either *Unc-5* or *fra* reveals that *Unc-5* is not expressed by the ISNb-projecting RP motor neurons either at or before the time that they form synapses on their ventral target muscles, whereas *fra* is strongly expressed by these cells (Figures 2A, 2D, and 2E). Thus, there is good agreement between the mRNA expression data and the differential genetic requirement for *Unc-5* and *fra* in different subsets of motor neurons that project to different regions along the dorsal/ventral axis. Together, our genetic and expression data suggest that Netrin-dependent guidance decisions made by dorsal, lateral, and ventral motor neurons are regulated by different receptor combinations and that the differential deployment of these receptors is controlled, at least in part, at the level of transcription.

Even-skipped Regulates Unc-5-Receptor Expression in Dorsal-ISN Motor Neurons

Despite extensive studies of how transcriptional codes and specific guidance receptors control motor-axon pathway selection, very few studies have established functional links between these codes and the regulation of guidance-receptor expression. Perhaps the clearest example of such a link is the demonstration that Lim1 regulates the expression of EphA4 receptors to control guidance of LMC motor neurons to appropriate domains in the limb [21]. The regulation of Robo-receptor expression in interneurons by the Lola transcription factor provides another example of functional

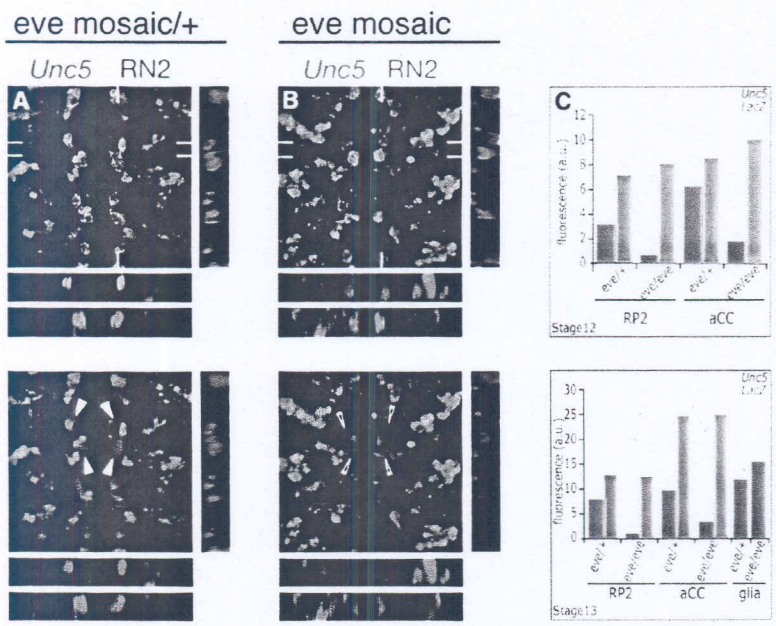

Figure 4. Endogenous *eve* Regulates *Unc-5*

Stage-13 mosaic *eve* mutant embryos (B) and their heterozygous siblings (A) were examined for *Unc-5* mRNA expression. The top panels show fluorescence RNA in situ with probes to *Unc-5* in green and LacZ antibody to identify the RP2 and aCC neurons in red. The bottom panels show RNA signals in green. Anterior is up in all panels. White hash marks indicate the positions of the XZ and YZ sections displayed below and to the right of the main XY panels, respectively. Two separate XZ sections are shown, one for aCC and one for RP2.

(A) A mosaic *eve*/+ heterozygous embryo shows clear expression of *Unc-5* mRNA in both aCC (green fluorescence units 6.04 ± 0.24 SEM in stage-12 embryos and 8.33 ± 0.20 SEM in stage-13 embryos) and RP2 (green fluorescence units 3.13 ± 0.15 SEM in stage-12 embryos and 7.46 ± 0.20 SEM in stage-13 embryos). Indeed, the cells are readily identified even in the absence of the LacZ probe (bottom panel, arrowheads point to RP2 and aCC).

(B) *eve* mosaic mutants show reduced or absent expression of *Unc-5* in both aCC (green fluorescence units 1.89 ± 0.13 SEM in stage-12 embryos and 2.57 ± 0.13 SEM in stage-13 embryos) and RP2 (green fluorescence units 0.85 ± 0.11 SEM in stage-12 embryos and 2.57 ± 0.13 SEM in stage-13 embryos). It is difficult to identify these neurons in the single label (bottom panel, empty arrowheads point to missing *Unc-5* mRNA in RP2 and aCC). However, other cells that are not mutant for *eve* show robust *Unc-5* expression (also [C], bottom panel, glia quantification).

(C) Quantification of fluorescence in stage-12 embryos (top panel) and stage-13 embryos (bottom panel). Genotypes for each cell analyzed are indicated on the x axis, and green or red fluorescence intensity is indicated on the y axis. Note that whereas the red fluorescence is comparable in both mutant and heterozygous embryos, the green fluorescence corresponding to *Unc-5* mRNA signal in RP2 and aCC is drastically reduced or at background levels in the mutants as compared to the heterozygous siblings. Green fluorescence (i.e., *Unc-5* mRNA) in nonmutant cells (glia, bottom panel) is comparable between mutant and heterozygous animals.

links between transcription factors and guidance-receptor expression [22].

There is a clear correlation between the expression and requirement of different combinations of Netrin receptors and the transcription-factor code controlling dorsal versus ventral motor-axon projection. Motor neurons that project in the dorsal ISN express the *eve* homeodomain transcription factor and both *fra* and *Unc-5*, whereas motor neurons that project in the ventral ISNb do not express *eve* (they instead express *lim-3*, *islet*, *Nkx6*, and *dHB9* [19, 23–25]) and express *fra* but not *Unc-5*. Given this positive correlation between *eve* and *Unc-5* expression, we next tested whether there is any link between *eve* function and *Unc-5* expression.

Previous studies have established that *eve* specifies the dorsal growth of ISN motor axons [5, 17]. For example, loss of *eve* function in just two dorsally projecting ISN motor neurons, RP2 and aCC, results in a failure of these neurons to project dorsally [17]. Interestingly, in these *eve* mosaic mutants, generated by rescuing *eve* null mutants with expression of *eve* under the control of a promoter element that recapitulates the entire *eve* expression pattern (except for the expression in the RP2, aCC, and pCC neurons [17]), ISN axons are frequently observed to inappropriately cross segment boundaries (Figures 3A–3C), a phenotype reminiscent of *Unc-5* mutants. In contrast to *eve* loss of function, misexpression of *eve* in ventrally projecting ISNb motor neurons redirects their axons dorsally, where they join and fasciculate with the dorsal branch of the ISN (Figures 3C and 3E) [5]. Importantly, neither loss nor gain of *eve* function dramatically alters cell fate; FasII expression and *eve* enhancer function are maintained in RP2 and aCC in *eve* mosaic mutants [17], and normal numbers of FasIII and Connectin positive ventral motor neurons are generated in *eve* gain-of-function embryos [5].

To test whether ectopic expression of *eve* influences *Unc-5* expression, we examined embryos misexpressing *eve* for *Unc-5* mRNA levels and observed a striking increase in the recruitment of *Unc-5*-expressing cells to the dorsal ISN (Figures 3G and 3H). We reasoned that if the observed upregulation of *Unc-5* contributes to the "dorsalization" of ISNb axons, ectopic expression of *Unc-5* should also change the normal behavior of ISNb axons and cause them to project more dorsally. This is indeed the case: *Unc-5* misexpression results in dramatic defects in the normal ventral guidance of ISNb, thereby redirecting these axons dorsally (Figures 3C and 3F). Importantly, the *Unc-5* gain-of-function phenotype is dependent on endogenous Netrin expression (Figure 3I). To further confirm the specificity of the *Unc-5* gain-of-function phenotype and to test the idea that the dorsalizing effect of *Unc-5* in the ISNb is due to *Unc-5* signaling, we misexpressed chimeric *Unc-5-Fra* and *Fra-Unc-5* receptors [10] and found that only *Fra-Unc-5* (consisting of *fra*'s ectodomain fused to the cytoplasmic domain of *Unc-5*) showed effects on the ISNb (Figure 3I). Furthermore, misexpression of full-length *fra* had no effect on the ISNb (data not shown).

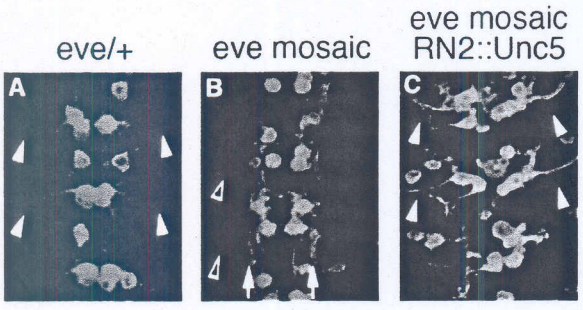

Figure 5. Expression of *Unc-5* Rescues the CNS-Exit Defects in *eve* Mosaic Mutants

Stage-16 *RN2Gal4::CD8GFP* embryos with the following genotypes: *eve* heterozygous (A), mosaic *eve* mutant (B), and mosaic *eve* mutant siblings expressing *Unc-5* (*RN2Gal4, UAS-HAUnc-5*) (C) labeled with antibodies to GFP to examine the aCC and RP2 projections.

(A) *eve* heterozygous embryos have wild-type aCC and RP2 axon projections toward the muscle field (arrowheads).

(B) In *eve* mosaic mutants, most aCC and RP2 motor neurons fail to exit the CNS (89%, n = 80 hemisegments), instead projecting longitudinally within the CNS (arrows). Occasionally, individual thin axons do exit the CNS (11% of the hemisegments, n = 80, empty arrowheads). Other defects include mispositioning of the RP2 and aCC cell bodies.

(C) Expression of *Unc-5* in RP2 and aCC in *eve* mosaic mutants results in increased motor-neuron exit (60% of the hemisegments, n = 100, arrowheads). Cell-body positioning remains defective. Anterior is up in all panels, and partial genotypes are indicated above each panel.

These results support the idea that the *Unc-5* gain of function in ISNb is specifically caused by ectopic *Unc-5* signaling in these neurons.

In contrast to misexpression of *eve*, where both ventral ISNb axons and lateral SNa axons project dorsally (Figure 3E), misexpression of *Unc-5* does not affect the lateral SNa (Figure 3F). This is perhaps not too surprising, because *Unc-5* is normally expressed in SNa. Given that *fra* is normally not expressed in the lateral SNa, we wondered whether *eve*'s ability to drive the SNa dorsally could be caused by the upregulation of the *fra* receptor in these neurons. To test this idea, we ectopically expressed *fra* in order to change the Netrin-receptor combination in SNa to the combination present normally in the more dorsal ISN (i.e., *fra* + *Unc-5*); however, this manipulation did not significantly affect SNa or any other motor projections, suggesting that the Netrin-receptor combination alone is not sufficient to convert lateral projections into dorsal projections (data not shown).

Although these observations suggest that ectopic *eve* can upregulate *Unc-5* expression, they do not establish whether *eve* normally functions to regulate *Unc-5*. To address this question, we again took advantage of the *eve* mosaic mutants, where *eve* is only mutant in two dorsally projecting ISN motor neurons per hemisegment: aCC and RP2 [17]. In wild-type animals or *eve*/+ heterozygotes, these neurons show robust expression of *Unc-5* mRNA (Figures 2B and 4A), whereas in *eve* mosaic mutants, there is a clear reduction in *Unc-5* mRNA expression in both aCC and RP2 (Figure 4B). Importantly, *Unc-5* expression is detected in other neurons and glia that are wild-type for *eve* at comparable levels to their heterozygous siblings (Figures 4A–4C). In contrast, expression of *fra* in *eve* mosaic mutants is not significantly affected (data not shown). To further test the relationship between *eve* and *Unc-5*, we examined whether the dorsal-extension defects in *eve* mosaic mutants could be "rescued" by expressing *Unc-5* just in RP2 and aCC. In contrast to *eve* mosaic mutants, where aCC and RP2 seldom exit the CNS (Figure 5B), targeted expression of *Unc-5* in these cells in *eve* mosaic mutants results in significant rescue of dorsal guidance (Figure 5C), a result that strongly supports the model that *Unc-5* functions downstream of *eve* to contribute to dorsal motor-axon guidance.

These results support a role for *Unc-5* in contributing to the translation of the dorsal versus ventral transcription-factor code into specific axon-guidance decisions, and provide one of the only examples of a functional link between transcriptional regulation of motor-axon projection and expression of specific axon-guidance receptors. Furthermore, to our knowledge, these findings are among the first to link transcriptional identity to guidance-receptor expression in single identified neurons. Changing the transcription-factor code or changing the combination of Netrin receptors expressed by ventrally projecting neurons both lead to more dorsal axon projections, albeit to different extents. Not surprisingly, manipulating the transcription-factor code leads to a more profound transformation of motor projections than does the alteration of a single guidance receptor. Clearly, many guidance receptors and adhesion molecules contribute to the pathfinding of individual motor projections; indeed, previous studies have implicated complementary and combinatorial influences of Semaphorin and Netrin ligands and of IgCam cell-adhesion molecules for the guidance and target selection of subsets of embryonic motor neurons [16]. Thus, the Netrin receptors are likely to represent only a fraction of the differentially regulated targets of the transcription-factor code. It will be interesting in the future to identify additional molecules that constitute the readout of transcriptional identity in motor neurons and to assess the similarities and differences between invertebrate and vertebrate systems.

Supplemental Data

Supplemental Data include detailed Experimental Procedures, two figures, and one table and are available with this article online at: http://www.current-biology.com/cgi/content/full/15/15/1413/DC1/.

Acknowledgments

We thank D. Garbe, M. Seeger, C. Doe, J. Skeath, A. Hidalgo, A. Kolodkin, N. Bonini, B. Dickson, M. Fujioka, J. Jaynes, and B. Edgar for various reagents and fly stocks. We thank Mathew Dalva and members of the Bashaw lab for many valuable discussions. J.P.L. was supported by a Human Frontier Science Program long-term postdoctoral fellowship. The authors were supported by grants from the National Institutes of Health to J.B.T. and by a Burroughs Wellcome Career Award and Whitehall Foundation Research Grant to G.J.B.

Received: April 23, 2005
Revised: June 17, 2005
Accepted: June 17, 2005
Published: August 9, 2005

References

1. Jessell, T.M. (2000). Neuronal specification in the spinal cord: Inductive signals and transcriptional codes. Nat. Rev. Genet. *1*, 20–29.
2. Shirasaki, R., and Pfaff, S.L. (2002). Transcriptional codes and the control of neuronal identity. Annu. Rev. Neurosci. *25*, 251–281.
3. Thor, S., and Thomas, J. (2002). Motor neuron specification in worms, flies and mice: Conserved and 'lost' mechanisms. Curr. Opin. Genet. Dev. *12*, 558–564.
4. Hobert, O., D'Alberti, T., Liu, Y., and Ruvkun, G. (1998). Control of neural development and function in a thermoregulatory network by the LIM homeobox gene lin-11. J. Neurosci. *18*, 2084–2096.
5. Landgraf, M., Roy, S., Prokop, A., VijayRaghavan, K., and Bate, M. (1999). *even-skipped* determines the dorsal growth of motor axons in *Drosophila*. Neuron *22*, 43–52.
6. Yu, T.W., and Bargmann, C.I. (2001). Dynamic regulation of axon guidance. Nat. Neurosci. *4* (*Suppl*), 1169–1176.
7. Harris, R., Sabatelli, L.M., and Seeger, M.A. (1996). Guidance cues at the Drosophila CNS midline: Identification and characterization of two Drosophila Netrin/UNC-6 homologs. Neuron *17*, 217–228.
8. Kolodziej, P.A., Timpe, L.C., Mitchell, K.J., Fried, S.R., Goodman, C.S., Jan, L.Y., and Jan, Y.N. (1996). *frazzled* encodes a Drosophila member of the DCC immunoglobulin subfamily and is required for CNS and motor axon guidance. Cell *87*, 197–204.
9. Mitchell, K.J., Doyle, J.L., Serafini, T., Kennedy, T.E., Tessier-Lavigne, M., Goodman, C.S., and Dickson, B.J. (1996). Genetic analysis of Netrin genes in Drosophila: Netrins guide CNS commissural axons and peripheral motor axons. Neuron *17*, 203–215.
10. Keleman, K., and Dickson, B.J. (2001). Short- and long-range repulsion by the Drosophila Unc5 netrin receptor. Neuron *32*, 605–617.
11. Leung-Hagesteijn, C., Spence, A.M., Stern, B.D., Zhou, Y., Su, M.W., Hedgecock, E.M., and Culotti, J.G. (1992). UNC-5, a transmembrane protein with immunoglobulin and thrombospondin type 1 domains, guides cell and pioneer axon migrations in C. elegans. Cell *71*, 289–299.
12. Leonardo, E.D., Hinck, L., Masu, M., Keino-Masu, K., Ackerman, S.L., and Tessier-Lavigne, M. (1997). Vertebrate homologues of C. elegans UNC-5 are candidate netrin receptors. Nature *386*, 833–838.
13. Hamelin, M., Zhou, Y., Su, M.W., Scott, I.M., and Culotti, J.G. (1993). Expression of the UNC-5 guidance receptor in the touch neurons of C. elegans steers their axons dorsally. Nature *364*, 327–330.
14. Hong, K., Hinck, L., Nishiyama, M., Poo, M.M., Tessier-Lavigne, M., and Stein, E. (1999). A ligand-gated association between cytoplasmic domains of UNC5 and DCC family receptors converts netrin-induced growth cone attraction to repulsion. Cell *97*, 927–941.
15. Colavita, A., and Culotti, J.G. (1998). Suppressors of ectopic UNC-5 growth cone steering identify eight genes involved in axon guidance in Caenorhabditis elegans. Dev. Biol. *194*, 72–85.
16. Winberg, M.L., Mitchell, K.J., and Goodman, C.S. (1998). Genetic analysis of the mechanisms controlling target selection: Complementary and combinatorial functions of netrins, semaphorins, and IgCAMs. Cell *93*, 581–591.
17. Fujioka, M., Lear, B.C., Landgraf, M., Yusibova, G.L., Zhou, J., Riley, K.M., Patel, N.H., and Jaynes, J.B. (2003). Even-skipped, acting as a repressor, regulates axonal projections in Drosophila. Development *130*, 5385–5400.
18. Van Vactor, D., Sink, H., Fambrough, D., Tsoo, R., and Goodman, C.S. (1993). Genes that control neuromuscular specificity in Drosophila. Cell *73*, 1137–1153.
19. Broihier, H.T., and Skeath, J.B. (2002). Drosophila homeodomain protein dHb9 directs neuronal fate via crossrepressive and cell-nonautonomous mechanisms. Neuron *35*, 39–50.
20. Nassif, C., Noveen, A., and Hartenstein, V. (1998). Embryonic development of the Drosophila brain. I. Pattern of pioneer tracts. J. Comp. Neurol. *402*, 10–31.
21. Kania, A., and Jessell, T.M. (2003). Topographic motor projections in the limb imposed by LIM homeodomain protein regulation of ephrin-A:EphA interactions. Neuron *38*, 581–596.
22. Crowner, D., Madden, K., Goeke, S., and Giniger, E. (2002). Lola regulates midline crossing of CNS axons in Drosophila. Development *129*, 1317–1325.
23. Broihier, H.T., Kuzin, A., Zhu, Y., Odenwald, W., and Skeath, J.B. (2004). Drosophila homeodomain protein Nkx6 coordinates motoneuron subtype identity and axonogenesis. Development *131*, 5233–5242.
24. Odden, J.P., Holbrook, S., and Doe, C.Q. (2002). Drosophila HB9 is expressed in a subset of motoneurons and interneurons, where it regulates gene expression and axon pathfinding. J. Neurosci. *22*, 9143–9149.
25. Thor, S., Andersson, S.G., Tomlinson, A., and Thomas, J.B. (1999). A LIM-homeodomain combinatorial code for motor-neuron pathway selection. Nature *397*, 76–80.